Antiviral Research 99 (2013) 172–179

Contents lists available at SciVerse ScienceDirect

Antiviral Research

journal homepage: www.elsevier.com/locate/antiviral

Inhibition of multiplication of the prototypic arenavirus LCMV by valproic acid

Ángela Vázquez-Calvo [a], Miguel A. Martín-Acebes [a], Juan-Carlos Sáiz [b], Nhi Ngo [c], Francisco Sobrino [a,*], Juan Carlos de la Torre [c]

[a] Centro de Biología Molecular "Severo Ochoa" (UAM-CSIC), Cantoblanco, Madrid, Spain
[b] Departamento de Biotecnología, Instituto Nacional de Investigación y Tecnología Agraria y Alimentaria (INIA), Madrid, Spain
[c] Department of Immunology and Microbial Science, The Scripps Research Institute, La Jolla, CA, United States

ARTICLE INFO

Article history:
Received 17 December 2012
Revised 24 April 2013
Accepted 24 May 2013
Available online 2 June 2013

Keywords:
Valproic acid
Antiviral
LCMV
Budding

ABSTRACT

Valproic acid (VPA), a short chain fatty acid commonly used for treatment of neurological disorders, has been shown to inhibit production of infectious progeny of different enveloped viruses including the prototypic arenavirus lymphocytic choriomeningitis virus (LCMV). In this study we have investigated the mechanisms by which VPA inhibits LCMV multiplication in cultured cells. VPA reduced production of infectious LCMV progeny and virus propagation without exerting a major blockage on either viral RNA or protein synthesis, but rather affecting the cell release and specific infectivity of LCMV progeny from infected cells. Our results would support the repurposing of VPA as a candidate antiviral drug to combat arenavirus infections.

1. Introduction

Arenaviruses are enveloped viruses with a bi-segmented, negative-strand (NS) RNA genome and a life cycle restricted to the cell cytoplasm (Buchmeier, 2007). Each RNA segment uses an ambisense coding strategy to direct the expression of two gene products in opposite orientations separated by a noncoding intergenic region. The large segment (L; 7.2 kb) encodes the L protein, an RNA-dependent RNA polymerase, and the small RING finger protein Z that is the counterpart of the matrix (M) protein found in many enveloped NS RNA viruses. The small segment (S; 3.5 kb) encodes the viral nucleoprotein (NP) and the glycoprotein (GP) precursor GPC. Co-translational cleavage of GPC by signal peptidase produces a 58 amino acid stable signal peptide (SP), and subsequent posttranslational processing of GPC by the cellular site 1 protease (S1P) generates the peripheral virion attachment protein GP1 and the fusion-active transmembrane protein GP2. Trimers of GP1/GP2 form the spikes that decorate the virus surface and mediate cell entry via receptor-mediated endocytosis (Buchmeier, 2007; Kunz, 2009, 2002). L and NP are the minimal trans-acting factors required for virus RNA replication and gene expression (Lee et al., 2000), whereas production of infectious particles also requires GP and Z (Lee et al., 2002) with the latter being the driving force of virus budding at the plasma membrane (Buchmeier, 2007).

Several arenaviruses, chiefly Lassa (LASV) and Junin (JUNV) cause hemorrhagic fever (HF) disease in humans representing an important public health concern within their endemic regions of West Africa (LASV) and Argentina (JUNV) (Geisbert and Jahrling, 2004; Peters, 2002). Moreover, evidence indicates that the globally distributed prototypic arenavirus LCMV is a neglected clinically relevant human pathogen (Barton et al., 2002; Jahrling and Peters, 1992; Mets et al., 2000). Concerns about arenavirus infections of humans are aggravated because the only existing vaccine, the JUNV live attenuated Candid1 strain, is licensed exclusively in Argentina and it does not protect against LASV induced disease. Likewise, existing anti-arenavirus therapy is limited to the use of the nucleoside analogue ribavirin, which is only partially effective and is associated with significant side effects (Snell, 1988). Therefore, it is important to develop novel antiviral strategies and drugs to combat human pathogenic arenaviruses.

We have shown that treatment of infected cells with valproic acid (VPA), a branched short-chain fatty acid commonly used for treatment of neurological disorders (Bruni and Wilder, 1979; Terbach and Williams, 2009), reduces the yield of infectious progeny for different enveloped viruses, which likely reflects an VPA-mediated impairment of lipid metabolism that may affect different steps of a virus life cycle (Vazquez-Calvo et al., 2011). In this study we have investigated the mechanisms whereby VPA inhibits multiplication of the prototypic arenavirus LCMV, an excellent model

* Corresponding author. Address: CBMSO, Nicolás Cabrera 1, UAM, 28049 Madrid, Spain. Tel.: +34 91 196 4493; fax: +34 91 196 4420.
E-mail address: fsobrino@cbm.uam.es (F. Sobrino).

0166-3542/$ - see front matter © 2013 Elsevier B.V. All rights reserved.
http://dx.doi.org/10.1016/j.antiviral.2013.05.012

to study basic aspects of the molecular and cell biology of HF arenaviruses. We present evidence that VPA treatment of LCMV-infected cells significantly reduced production of LCMV infectious progeny without significantly affecting levels of viral RNA and protein synthesis but rather interfering with both cell release and specific infectivity of virion particles.

2. Materials and methods

2.1. Cells and viruses

HEK293T, Vero E6 and BHK-21 cells were grown in Dulbecco's modified Eagle's medium (DMEM; Invitrogen) containing 10% fetal bovine serum (FBS), 2 mM L-glutamine, 100 mg/ml streptomycin, and 100 U/ml penicillin. Stocks of LCMV Armstrong 53b strain (LCMV Arm) and the tri-segmented recombinant LCMV expressing GFP (r3LCMV-GFP) (Emonet et al., 2009) were produced by infecting (moi = 0.1) BHK-21 cells and harvesting the tissue culture supernatant (TCS) at 72 h post-infection (pi). After clarification (10,000*g*/4 °C/5 min) TCS were stored at −80 °C.

2.2. Infections and virus titrations

BHK-21 cells were infected with LCMV at the indicated moi. After 90 min adsorption time, the viral inoculum was removed, cell monolayers washed twice with DMEM and fresh medium containing 2% FBS and different concentrations of valproic acid (VPA), or vehicle, was added; this time point was considered 0 h (p.i). LCMV titers (focus forming unit – FFU/ml) were determined by immunofocus assay (Battegay, 1993). Briefly, serial virus dilutions were used to infect Vero E6 cell monolayers in a 96-well plate, and at 20 h p.i., cells were fixed by using 4% formaldehyde in phosphate-buffered saline (PBS), permeabilized by treatment with 0.3% Triton X-100 in PBS containing 3% bovine serum albumin (BSA) and stained with the 1.1.3 mouse monoclonal antibody to NP and an Alexa Fluor 568-labeled anti-mouse secondary antibody (Molecular Probes). In the case of r3LCMV-GFP virus titer was determined based on GFP expression. Alternatively, virus titers were also determined by standard plaque assay in semisolid agar medium, as described (Vazquez-Calvo et al., 2011).

2.3. Analysis of viral RNA synthesis by Northern blot

Total cellular RNA was isolated by using TriReagent (Molecular Research Center) an equal amounts of RNA from each sample analyzed by Northern blot hybridization using a ^{32}P-radiolabeled NP DNA probe as described (Cornu and de la Torre, 2001).

2.4. Drug treatment

Stock solutions (100 mM) of VPA (Sigma) were prepared freshly in DMEM and used at final concentration of 2, 5 or 10 mM, as previously described (Vazquez-Calvo et al., 2011). In the case of infected cells, the drug was added after adsorption (90 min).

2.5. Cytotoxicity assay

The effect of VPA on cell viability was determined using the CellTiter-Glo Luminiscent Cell Viability assay (Promega). Briefly, BHK-21 cells were seeded in 6-well plates and treated with increasing concentrations of VPA (0–200 mM). After 48 or 72 h cells were incubated with CellTiter-Glo reagent and the assay was performed according to the manufacturer's recommendations. The concentration of VPA causing 50% toxicity (TC_{50}) was calculated.

2.6. Minigenome assay

BHK-21 cells were transfected with pol1MG-CAT, pCAGGS-NP and pCAGGS-L as described (Lee et al., 2000). After 5 h transfection, the medium was replaced with fresh medium containing different concentrations of VPA. Levels of chloramphenicol acetyltransferase (CAT) protein in cell lysates at 48 h post-transfection were determined by enzyme-linked immunosorbent assay (ELISA) using a CAT ELISA kit (Roche catalog No. 11363727001).

2.7. Z-mediated budding assay

293T cells were transfected with 0.1 μg of pCAGGS-Z-Flag (pC-Z) (Urata et al., 2012) or the empty pCAGGS (pC-E) control plasmid using Lipofectamine 2000 (Invitrogen) (2 μl/μg DNA). After 5 h transfection the medium was replaced with fresh media containing VPA (0, 2, 5 or 10 mM) and 48 h later virus-like particles (VLP) containing TCS and cells were harvested. After removal of cell debris by centrifugation (1500*g*; 5 min), VLPs were collected by ultracentrifugation (100,000*g*; 30 min at 4 °C) through a 20% sucrose cushion. Cells and VLPs were re-suspended in lysis buffer (1% NP-40, 50 mM Tris–HCl [pH 8.0], 62.5 mM EDTA, 0.4% sodium deoxycholate) and their proteins analyzed by SDS–PAGE, followed by western blotting (WB).

2.8. Western blot

Cell lysates, VLPs or viral particles samples were resolved by SDS–PAGE, followed by western blot using a rabbit polyclonal serum to the Flag epitope (Cayman catalog No. 162150), or monoclonal antibodies (MAb) to actin (sc-1616-R; Santa Cruz), LCMV NP (MAb 1.1.3), or LCMV GP-2 (MAb 83.6) (Buchmeier et al., 1981; Weber and Buchmeier, 1988) as the first antibody, and horseradish peroxidase (HRP)-conjugated either anti-rabbit (Flag) or anti-mouse IgG as the second antibody.

2.9. Virus purification

BHK-21 cells were infected (moi = 1) with LCMV and treated or not with 10 mM VPA. Culture supernatants were harvested at 24 h p.i. and clarified at 2000 rpm for 10 min at 4 °C in a Sorvall centrifuge using a SS34-V1 rotor. A further clarification step of cell supernatants was performed at 10,000 rpm (30 min at 4 °C) in a Beckman Coulter Optima L-100 XP ultracentrifuge using an SW27 rotor. Viral particles were collected by centrifugation through a 20% sucrose cushion in PBS (35,000 rpm for 2.5 h at 4 °C) using a TST41.14 rotor. Viral particles-containing pellet was re-suspended in 40 μl of PBS and stored at 4 °C.

2.10. Transmission electron microscopy (TEM)

LCMV and mock-infected control cell monolayers, grown on 100 mm ∅ dishes, were washed three times with Sörensen's phosphate buffer (0.1 M, pH 7.4) and fixed 1 h at room temperature (RT) in 4% parafirmaldehyde-2% glutaraldehyde in Sörensen buffer. Cells were scrapped and post-fixed in 1% osmium tetroxide-1% potassium ferricyanide for 1 h at 4 °C, washed three times with bi-distilled water and treated with 0.15% tanic acid in phosphate buffer pH 7.4 for 1 min. Cells were washed with the buffer and with bi-distilled water and samples were stained with 2% uranyl acetate for 1 h at RT. After three washes with bi-distilled water the samples were dehydrated in ethanol and embedded in TAAB 812 resin (TAAB Laboratories). For negative staining, purified LCMV virions were fixed with 1% glutaraldehide. Samples were adsorbed for 3 min to copper grids coated with collodion–carbon and ionized. Grids were negatively stained with 2% uranyl acetate

and air-dried. To determine the viral particle concentration, two independent LCMV preps were incubated with a known concentration of polystyrene latex particles (120 nm, Agar Scientific Ltd.), negatively stained and scored. Samples were examined using a Jeol JEM-1010 electron microscope (Jeol) operating at 80 kV and images were acquired using a digital camera TemCam-F416 (TVIPS).

2.11. Data analysis

One-way analysis of the variance was performed with statistical package SPSS 19.0 (SPSS, Inc.) for Windows. Data are presented as mean ± standard deviation. Differences were considered statistically significant when $P < 0.05$.

3. Results

3.1. Effect of VPA on LCMV multiplication in BHK-21 cells

We first evaluated the impact of VPA treatment on the viability of BHK-21 cells. VPA exhibited 50% toxic concentration (TC_{50}) of 33.42 mM during 48 h treatment or 28.43 mM during 72 h treatment (Fig. 1). At 10 mM VPA had no noticeable effects on cell viability after either 48 or 72 h of treatment and thereby we selected this VPA concentration for further experiments. Then, we examined the effect of VPA on LCMV multiplication following infection of BHK-21 cells at low (0.01) moi. To facilitate virus detection in infected cells we used a recombinant tri-segmented LCMV that expresses GFP (r3LCMV-GFP) (Emonet et al., 2009). Treatment of infected cells with VPA (10 mM) did not have any noticeable effect on cell survival over the duration (72 h) of the experiment but resulted in a large reduction in the numbers of GFP positive cells at 48 and 72 h p.i. (Fig. 2A and B). VPA induced reduction in the number of virus-derived GFP positive cells correlated with a drastic reduction in production of infectious progeny of both r3LCMV-GFP (Fig. 3A) and wild type LCMV (LCMV-WT) (Fig. 3B). We obtained similar results following infections at higher (0.5) moi (data not shown). To asses a possible direct effect of VPA on the infectivity of LCMV particles, as it has been described for other antiviral drugs against enveloped viruses (Wolf et al., 2010), we treated equal numbers of FFU of r3LCMV-GFP (Fig. 4A) or WT LCMV (Fig. 4B) with VPA (10 mM) or vehicle at 37 °C for 30 and 60 min, followed by determination of virus infectivity. Results from this experiment indicated that VPA did not have any noticeable virucidal effect on either r3LCMV-GFP or LCMV-WT.

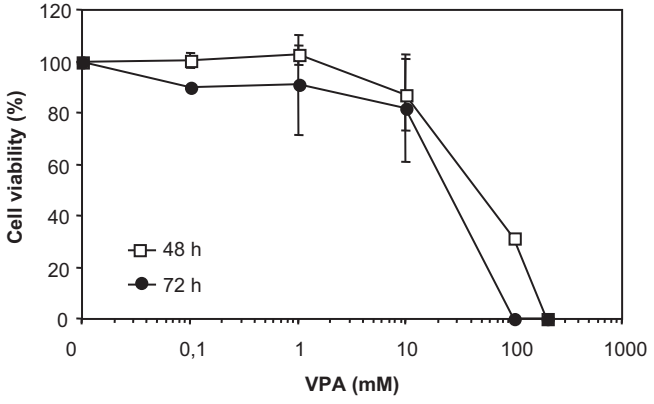

Fig. 1. Effect of VPA on BHK-21 cell viability. BHK-21 cells were grown for 48 or 72 h in the presence of the indicated concentrations of VPA and cell viability determined by using the CellTiter-Glo Kit. Average and SD of two replicates are shown.

To investigate the dose-dependency of the anti-LCMV activity of VPA, we infected (moi = 0.01) BHK-21 cells in the presence of increasing concentrations of VPA and at 48 h p.i. we determined virus titers in TCS. VPA inhibited production of infectious LCMV progeny in a dose dependent manner with a half maximal inhibitory concentration (IC_{50}) of 0.058 mM (Fig. 5) and a selectivity index ($SI = TC_{50}/IC_{50}$) of 576.2.

3.2. Effect of VPA on viral RNA synthesis

We next examined whether VPA treatment had an effect on LCMV RNA synthesis. For this, we used Northern blot (NB) analysis to conduct a time-course study of LCMV RNA synthesis following infection of BHK-21 cells at low (0.1) moi in the absence or presence (10 mM) of VPA (Fig. 6A). LCMV RNA genome replication (S RNA) and transcription (NP mRNA) exhibited similar kinetics and peak levels in both vehicle- and VPA-treated LCMV-infected cells, however the S RNA levels in the VPA-treated infected cells were slighter lower than those observed in vehicle-treated at 24 h p.i. Consistent with these observations, VPA treatment did not significantly affect the expression levels of a CAT reporter gene produced by an LCMV minigenome (Fig. 6B).

3.3. Effect of VPA treatment on arenavirus budding

Our observation that VPA had a robust inhibitory effect on production of LCMV infectious progeny without significantly affecting viral RNA synthesis, led us to consider that VPA might have an effect in virus budding. As the Z protein has been shown to be the main driving force of arenavirus budding (Pérez et al., 2003), we examined the effect of VPA on Z-mediated budding using a cell-based assay previously described (Pérez et al., 2003). For this, we transfected 293T cells with pC-Z-Flag and 5 h later the medium was replaced with fresh medium containing increasing concentrations of VPA. At 48 h post-transfection we collected TCS and prepared cell lysates. Z-containing VLPs were isolated from TCS as described in Section 2. Levels of Z in cell lysates and VLP preparations were determined by WB using an antibody to Flag (Fig. 7A). We observed that VPA at the lowest concentration used (2 mM) caused about 50% reduction in Z-mediated budding, and this inhibitory effect did not augment in cells treated with higher (5 and 10 mM) VPA concentration (Fig. 7B). Cellular levels of Z were slightly reduced in non-treated compared to VPA-treated cells, which likely reflects a higher rate of Z budding in VPA non-treated cells. It should be noted that we have previously documented that Z mutants impaired in budding activity accumulate within cells to higher levels than wt Z.

3.4. Effect of VPA on morphology and infectivity of cell released LCMV particles

Our observation that VPA inhibited Z-mediated budding led us to examine whether VPA interfered with viral particle release. To this end we infected (moi = 1) with LCMV BHK-21 cells treated or not with VPA (10 mM) and at 24 h p.i. we collected tissue culture supernatants (TCS) and prepared cells for transmission electron microscopy (TEM).

Both vehicle and VPA-treated LCMV-infected cells displayed areas rich in vesicles (Fig. 8A) containing structures with features similar to those previously documented to correspond to intracellular LCMV particles (Martin et al., 2010) (Fig. 8B), suggesting that VPA did not exert a major blockade on intracellular assembly of LCMV. We next examined whether the morphology, size and infectivity of LCMV progeny particles released from infected cells were affected by VPA treatment. For this, viral particles released to TCS from LCMV-infected cells, treated or not with VPA, were

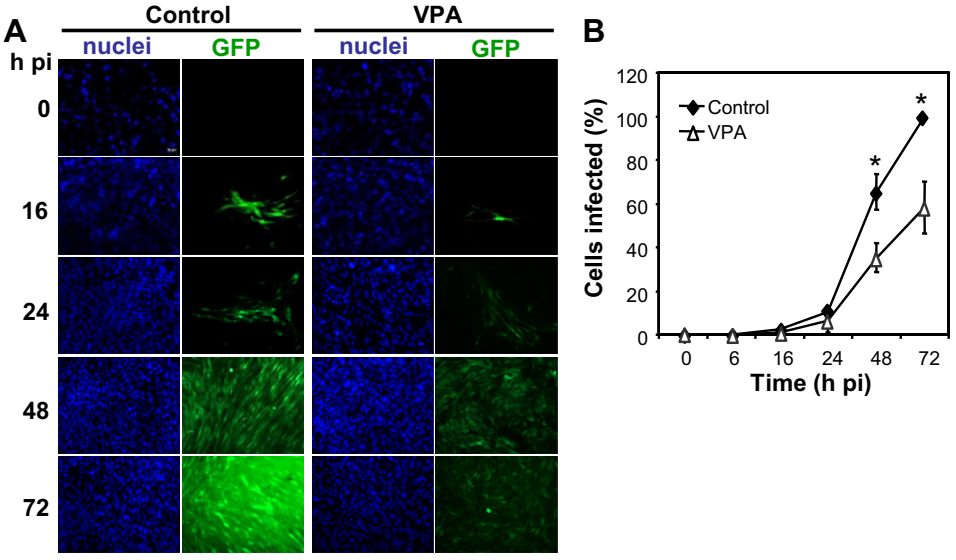

Fig. 2. Effect of VPA on r3LCMV-GFP propagation. (A) BHK-21 cells were infected with r3LCMV-GFP (moi = 0.01) as described in Section 2. After the adsorption, fresh medium without or with VPA (10 mM) was added. At the indicated times p.i. cells were fixed and GFP expression detected by epifluorescence. Cell nuclei were stained with DAPI (blue). Representative fields are shown for each time point and infection. (B) For each time point, the percentage of GFP positive (infected) cells is shown. Statistically significant differences between control and VPA-treated samples are indicated by an asterisk ($P \leqslant 0.05$). (For interpretation of the references to colour in this figure legend, the reader is referred to the web version of this article.)

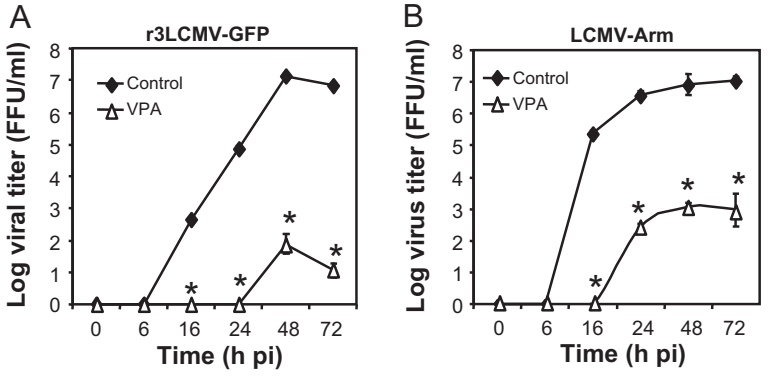

Fig. 3. VPA inhibits production of infectious LCMV progeny. (A and B) Effect of VPA on production of LCMV infectious progeny. BHK-21 cells were infected (moi = 0.01) with either r3LCMV-GFP (A) or LCMV-WT (B). After the adsorption, fresh medium without or with VPA (10 mM) was added, and virus titers in tissue culture supernatants (TCS) determined by immunofocus assay at the indicated times p.i.

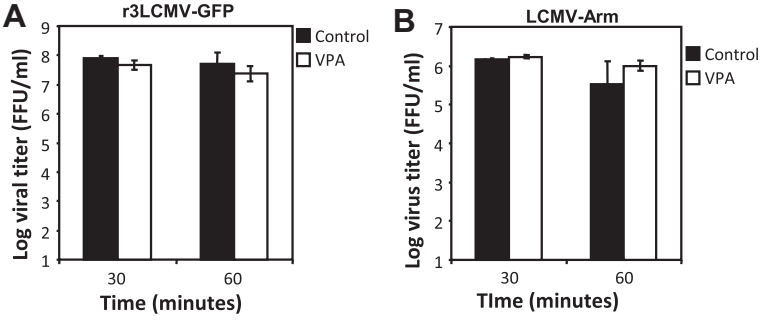

Fig. 4. VPA has not a virucidal effect on LCMV. (A and B) r3LCMV-GFP (2×10^5 FFU) (A) or LCMV-WT (2×10^5 FFU) (B) were incubated without or with VPA (10 mM) at 37 °C for 30 or 60 min. Then, serial virus dilutions were used to infect Vero E6 cell monolayers in a 96-well plate and virus infectivity determined by immunofocus assay as is described in Section 2. Statistically significant differences between control and VPA are indicated by an asterisk ($P \leqslant 0.05$).

concentrated and examined by TEM using negative staining. In both cases, viral particles showed similar morphologies (Fig. 8C) and sizes (Fig. 8D) that were consistent with those previously reported (Rodrigo et al., 2011). TCS infectious titers derive from infected cells in the presence or absence of VPA were 1.40×10^4 and 3.95×10^6 PFU/ml, respectively. VPA treatment caused about 280-fold decreased in TCS infectivity by only about 2-fold reduction in the numbers of total virion particles released (Fig. 8E). VPA-mediated reduced incorporation of GP-1 into released particles could account for the large reduction in the specific infectivity

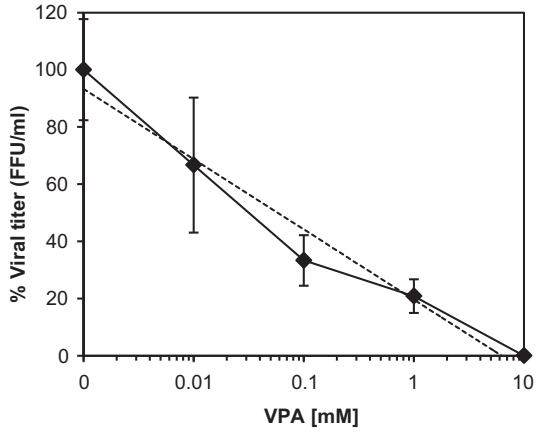

Fig. 5. VPA IC_{50}. BHK-21 cells were infected with LCMV-WT as in Fig 3. After the adsorption, fresh medium containing 0, 0.1, 1 or 10 mM VPA was added. Virus titers in TCS were determined by immunofocus assay at 48 h p.i. IC_{50} value was determined from the curve fitting (discontinued line).

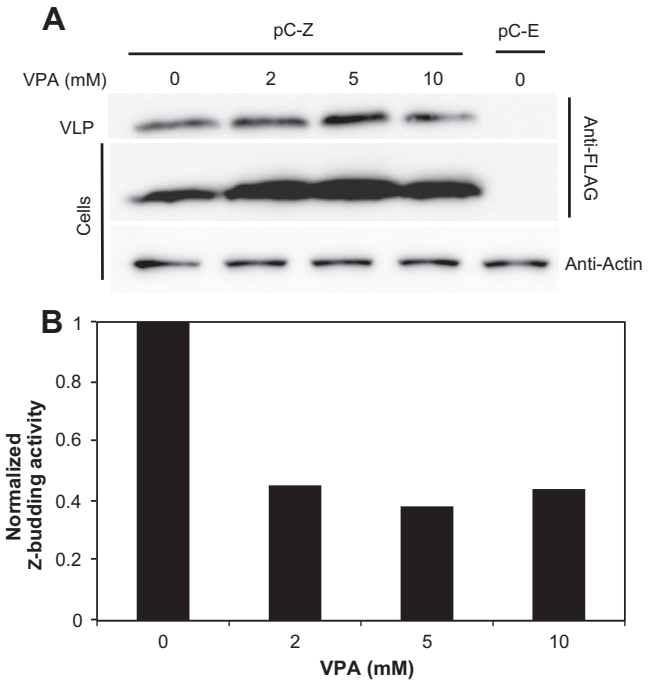

Fig. 7. VPA inhibits Z-mediated budding. (A) 293T cells were transfected with pC-Z or pC-E in the presence of the indicated VPA concentrations and at 48 h post-transfection TCS were collected and total cell lysates prepared. VLPs were isolated from TCS as described (Urata et al., 2009). Levels of Z in cell lysates and VLPs were determined by western blot using an anti-Flag antibody. Levels of actin in cell lysates were used as loading control. (B) Normalized levels of Z budding.

of the released particles. To examine this question we determined by Western blot the GP2/NP ratios in particles isolated from LCMV-infected cells in the absence or presence of VPA (Fig. 8F). Because the availability of antibodies that work in Western blot, we used GP2 as a surrogate of the levels of GP1 present in particles released into the supernatant of LCMV-infected cells. Treatment with VPA did not affect significantly the GP2/NP ratio compared to VPA untreated LCMV-infected cells.

4. Discussion

In a previous study we reported that VPA exhibits a broad-spectrum antiviral reflected by its ability to inhibit multiplication of enveloped viruses belonging to five different viral families. VPA appears to exert its broad-spectrum antiviral activity via different mechanisms. Thus, we showed that VPA blocked WNV, but not VSV, RNA replication and protein synthesis, whereas VPA

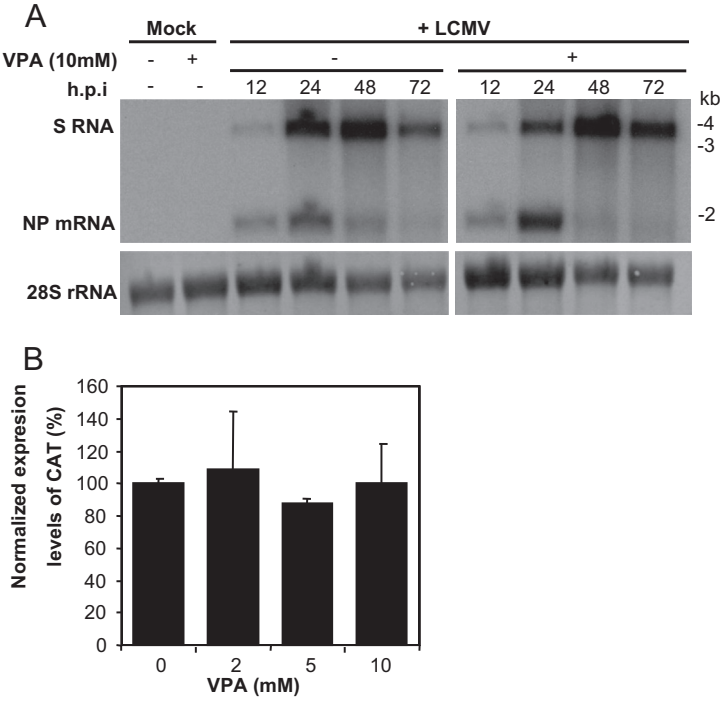

Fig. 6. VPA does not inhibit LCMV RNA synthesis. (A) BHK-21 cells were infected with LCMV-WT (moi = 0.1) as described Fig 3. After adsorption time, fresh medium without or with VPA (10 mM) was added. At the indicated times p.i. total cellular RNA was isolated and equal amounts from each sample analyzed by Northern blot hybridization using a NP ^{32}P-dsDNA to assess levels of LCMV RNA replication (S RNA) and transcription (NP mRNA). (B) BHK-21 cells were transfected with the plasmid components of the LCMV MG rescue system (see Section 2) in the presence of the indicated VPA concentrations, and at 48 h post-transfection total cell extracts were processed to determine expression levels of CAT as described in Section 2 (Cornu and de la Torre, 2001).

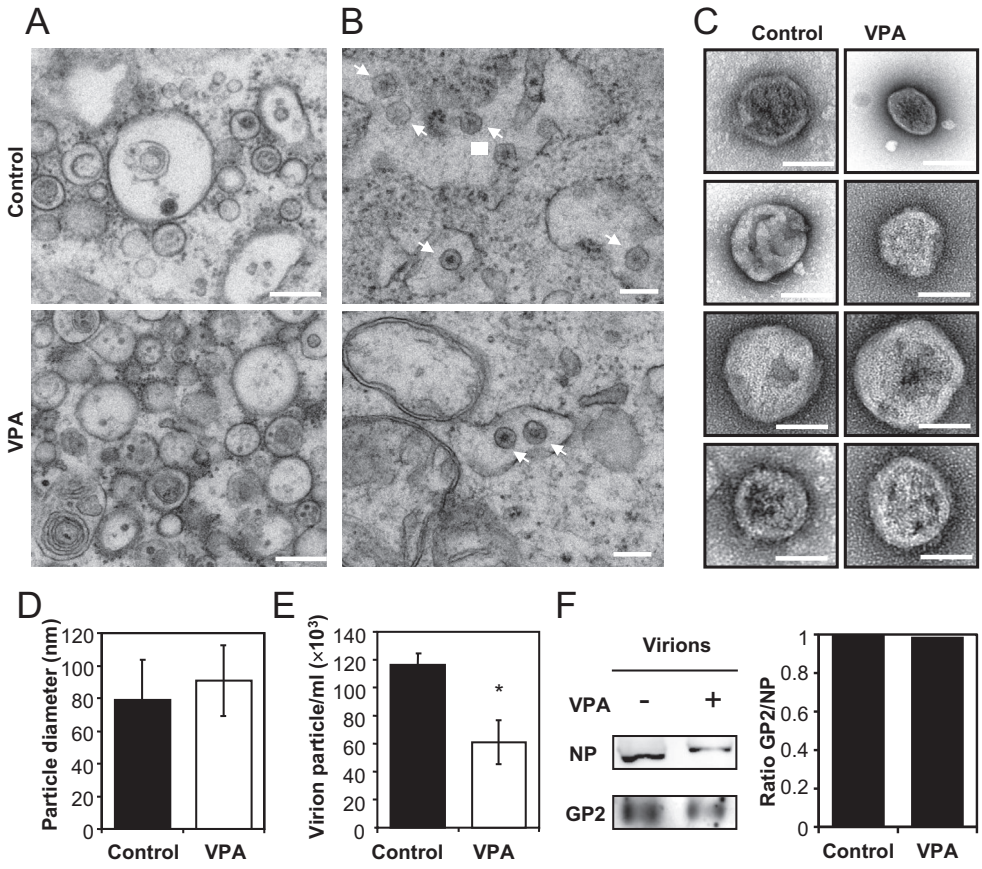

Fig. 8. VPA reduces the number of viral particles released. (A and B) BHK-21cells infected with LCMV (moi = 1) were fixed and processed for TEM at 24 h p.i. (A) VPA does not inhibit the formation of virus-induced vesicles in infected cells. Bar: 200 nm. (B) LCMV-like particles in vesicles from infected cells. (C) Viral particles from supernatants of cells infected as in (A) and were purified, negative stained and observed by TEM. Bar: 50 nm. (D) The diameter of viral particles purified as in (C) was measured for control and VPA treated samples. (E) Viral particle concentration was determined by quantitative TEM in samples purified as in (C). (F) The amount of NP and GP2 in particles isolated from supernatants of LCMV-infected cells was determined by Western blot using appropriated antibodies. The graph represents the ratios GP2/NP. Statistically significant differences between control and VPA are indicated by an asterisk ($P \leqslant 0.05$).

treatment caused a drastic reduction on the release and stability of VSV particles (Vazquez-Calvo et al., 2011). In this report we have investigated the mechanisms whereby VPA inhibits multiplication of the prototypic arenavirus LCMV. Our results have shown that VPA inhibited very robustly production of infectious LCMV progeny (Figs. 2 and 3) but minimally interfered with viral RNA synthesis in virus-infected cells (Fig. 6A). Accordingly, VPA treatment did not affect levels of a reported gene whose expression was driven by an LCMV minigenome system (Fig. 6B). At 24 h p.i. the ratio S/NPmRNA in LCMV-infected cells was consistently slightly lower in VPA-treated cells compared to untreated control cells. This likely reflected the effect of VPA treatment on production of infectious progeny, which affected the speed of virus propagation throughout the cell monolayer following infection at low (0.01) moi. The faster propagation of LCMV in VPA untreated cells resulted in a slightly faster peak of levels of genome and antigenome S RNA species, which was accompanied by the initiation of down-regulation of viral transcription.

VPA has been documented to exert different effects on cells including: (i) interruption of γ-amino butyric acid (GABA) signalling; (ii) inhibition of histone deacetylases (HDAC); (iii) modulation of sodium channel activity; inhibition of glycogen synthase kinase 3; and (v) disruption of membrane lipids metabolism, including that of phosphatidylinositol (Shaltiel et al., 2004; Tokuoka et al., 2008; Venkataramani et al., 2010; Wittenburg et al., 2010; Xu et al., 2007). Therefore, VPA-mediated interference with a variety of cellular processes may be at the root of the anti-LCMV activity of VPA. However, inhibition of HDAC is unlikely to mediate the anti-LCMV activity of VPA as we have shown that the HDAC trichostatin A did not affect LCMV multiplication (Vazquez-Calvo et al., 2011). On the other hand, a number of studies have documented that VPA affects the lipid composition of cellular membranes (Shaltiel et al., 2004; Terbach and Williams, 2009; Tokuoka et al., 2008; Xu et al., 2007) and it has been proposed that VPA treatment could alter VSV particle composition as to render extracellular particles with reduced stability (Vazquez-Calvo et al., 2011).

Arenaviruses replication is confined to the cytoplasm of infected cells and budding of progeny virus occurs mainly at the plasma membrane (Buchmeier, 2007). Budding of arenaviruses from the plasma membrane involves the association of the virus ribonucleoprotein core with host-derived membranes enriched for viral surface GPs (Pérez et al., 2003), a process that is driven by the Z protein, which has been shown to be the driving force of arenavirus budding (Capul and de la Torre, 2008; Pérez et al., 2003; Strecker et al., 2003; Urata et al., 2006). Z-mediated budding involves its interaction with host cell proteins including members of the multivesicular body pathway (Pérez et al., 2003; Strecker et al., 2003; Urata et al., 2006), and these interactions required myristoylation of Z at position G2 that promotes Z association with membranes (Perez et al., 2004). Therefore, VPA-mediated effects on lipid metabolism may have also contributed to impaired Z budding efficiency (Fig. 7) in our cell-based assay (Pérez et al., 2003). It should be noted that VPA did not exhibit a typical linear

dose-dependent inhibition of either production of LCMV infectious progeny (Fig. 5) or Z budding activity (Fig. 7). The exact mechanisms by which VPA inhibits LCMV multiplication remain to be determined and it may involve a complex combination of interactions that would exert their full potential inhibitory activity only once VPA reaches a threshold concentration in cells, which could account for its non-linear dose-dependent inhibitory activity.

VPA treatment did not affect the morphology and size of released viral particles (Fig. 8), but consistent with the effect of VPA on Z-mediated budding, the numbers of viral particles released to the medium from LCMV-infected cells was significantly lower (about 2-fold reduction) in VPA-treated cells compared to non-treated controls (Fig. 7E). This effect however cannot account for the magnitude of the inhibitory effect exerted by VPA treatment on production of infectious progeny (about 280-fold reduction), suggesting that VPA affected not only the efficiency of particle release but also their specific infectivity, a finding similar to that described for VSV infection (Vazquez-Calvo et al., 2011). The effect of VPA on the specific infectivity of released virus particles was not related to reduced incorporation of surface viral GPs into the viral particles (Fig. 8F). The previously commented alteration of cellular lipid metabolism induced by VPA probably results in alterations of the lipidic composition of the cellular membranes from which LCMV acquires its envelope. These alterations could be behind the reduction of infectivity of released LCMV particles in VPA-treated cells here reported.

The live-attenuated Candid1 vaccine strain of JUNV is only licensed for use in Argentina and it does not protect against LASV infection. Likewise current anti-arenavirus therapy is limited to an off-labelled use of ribavirin that is only partially effective and associated with significant side effects (Borio et al., 2002). The results described in this work raise the possibility of a therapeutic antiviral use of VPA. The SI of a compound is considered as a good predictor of the feasibility for its development into a potential candidate antiviral drug (Li et al., 2005). Notably, VPA exhibited a SI of 576.2 for LCMV, which supports to consider VPA as a good antiviral drug candidate against arenaviruses. It should be noted that VPA is currently being used for epilepsy treatment and its therapeutic dose range (50–100 mg/kg) results in concentrations of VPA in plasma of 0.3–0.6 mM (Cramer et al., 1986; Kanner, 2003), which are significantly higher than the IC_{50} value we determined for LCMV (0.058 mM). Therefore, at its currently used therapeutic dose range VPA might exert an in vivo antiviral effect against arenaviruses.

5. Conclusions

The anticonvulsant VPA, a drug currently used for treatment of neurological disorders in humans, reduced multiplication of LCMV without exerting a major blockage on either viral RNA or protein synthesis. But rather VPA affected both the release of viral particles from infected cells and the specific infectivity of released virions. The results presented in this report would support the repurposing of VPA as a candidate antiviral drug to combat arenavirus infections.

Acknowledgements

We thank M.T. Rejas for advice in the TEM studies and B. Cubitt for excellent technical assistance.

This work was supported by Spanish grants BIO2008-0447-C03-01 and BIO2011-24351, and by an institutional grant from Fundación Ramón Areces, and by NIH AI077719 JCT and by RTA2011-00036. MAMA is the recipient of JAE-Doc fellowship from CSIC.

Appendix A. Supplementary data

Supplementary data associated with this article can be found, in the online version, at http://dx.doi.org/10.1016/j.antiviral.2013.05.012.

References

Barton, L.L., Mets, M.B., Beauchamp, C.L., 2002. Lymphocytic choriomeningitis virus: emerging fetal teratogen. Am. J. Obstet. Gynecol. 187, 1715–1716.
Battegay, M., 1993. Quantification of lymphocytic choriomeningitis virus with an immunological focus assay in 24 well plates. ALTEX 10, 6–14.
Borio, L., Inglesby, T., Peters, C.J., Schmaljohn, A.L., Hughes, J.M., Jahrling, P.B., Ksiazek, T., Johnson, K.M., Meyerhoff, A., O'Toole, T., Ascher, M.S., Bartlett, J., Breman, J.G., Eitzen Jr., E.M., Hamburg, M., Hauer, J., Henderson, D.A., Johnson, R.T., Kwik, G., Layton, M., Lillibridge, S., Nabel, G.J., Osterholm, M.T., Perl, T.M., Russell, P., Tonat, K., 2002. Hemorrhagic fever viruses as biological weapons: medical and public health management. JAMA 287, 2391–2405.
Bruni, J., Wilder, B.J., 1979. Valproic acid. Review of a new antiepileptic drug. Arch. Neurol. 36, 393–398.
Buchmeier, M.J., Peters, C.J., de la Torre, J.C., 2007. In: Arenaviridae: The Viruses and Their Replication, . fifth ed.. Fields Virology fifth ed., vol. 2 Lippincott Williams & Wilkins, Philadelphia, PA.
Buchmeier, M.J., Lewicki, H.A., Tomori, O., Oldstone, M.B., 1981. Monoclonal antibodies to lymphocytic choriomeningitis and pichinde viruses: generation, characterization, and cross-reactivity with other arenaviruses. Virology 113, 73–85.
Capul, A.A., de la Torre, J.C., 2008. A cell-based luciferase assay amenable to high-throughput screening of inhibitors of arenavirus budding. Virology 382, 107–114.
Cornu, T.I., de la Torre, J.C., 2001. RING finger Z protein of lymphocytic choriomeningitis virus (LCMV) inhibits transcription and RNA replication of an LCMV S-segment minigenome. J. Virol. 75, 9415–9426.
Cramer, J.A., Mattson, R.H., Bennett, D.M., Swick, C.T., 1986. Variable free and total valproic acid concentrations in sole- and multi-drug therapy. Ther. Drug Monit. 8, 411–415.
Emonet, S.F., Garidou, L., McGavern, D.B., de la Torre, J.C., 2009. Generation of recombinant lymphocytic choriomeningitis viruses with trisegmented genomes stably expressing two additional genes of interest. Proc. Natl. Acad. Sci. USA 106, 3473–3478.
Geisbert, T.W., Jahrling, P.B., 2004. Exotic emerging viral diseases: progress and challenges. Nat. Med. 10, S110–S121.
Jahrling, P.B., Peters, C.J., 1992. Lymphocytic choriomeningitis virus. A neglected pathogen of man. Arch. Pathol. Lab. Med. 116, 486–488.
Kanner, A.M., 2003. The pharmacology of parenteral valproate. Epilepsy Curr. 3, 109–111.
Kunz, S., 2009. Receptor binding and cell entry of Old World arenaviruses reveal novel aspects of virus–host interaction. Virology 387, 245–249.
Kunz, S., Borrow, P., Oldstone, M.B., 2002. Receptor structure, binding, and cell entry of arenaviruses. Curr. Top. Microbiol. Immunol. 262, 111–137.
Lee, K.J., Novella, I.S., Teng, M.N., Oldstone, M.B., de La Torre, J.C., 2000. NP and L proteins of lymphocytic choriomeningitis virus (LCMV) are sufficient for efficient transcription and replication of LCMV genomic RNA analogs. J. Virol. 74, 3470–3477.
Lee, K.J., Pérez, M., Pinschewer, D.D., de la Torre, J.C., 2002. Identification of the lymphocytic choriomeningitis virus (LCMV) proteins required to rescue LCMV RNA analogs into LCMV-like particles. J. Virol. 76, 6393–6397.
Li, S.Y., Chen, C., Zhang, H.Q., Guo, H.Y., Wang, H., Wang, L., Zhang, X., Hua, S.N., Yu, J., Xiao, P.G., Li, R.S., Tan, X., 2005. Identification of natural compounds with antiviral activities against SARS-associated coronavirus. Antiviral Res. 67, 18–23.
Martin, V., Abia, D., Domingo, E., Grande-Perez, A., 2010. An interfering activity against lymphocytic choriomeningitis virus replication associated with enhanced mutagenesis. J. Gen. Virol. 91, 990–1003.
Mets, M.B., Barton, L.L., Khan, A.S., Ksiazek, T.G., 2000. Lymphocytic choriomeningitis virus: an underdiagnosed cause of congenital chorioretinitis. Am. J. Ophthalmol. 130, 209–215.
Pérez, M., Craven, R.C., de la Torre, J.C., 2003. The small RING finger protein Z drives arenavirus budding: implications for antiviral strategies. Proc. Natl. Acad. Sci. USA 100, 12978–12983.
Perez, M., Greenwald, D.L., de la Torre, J.C., 2004. Myristoylation of the RING finger Z protein is essential for arenavirus budding. J. Virol. 78, 11443–11448.
Peters, C.J., 2002. Human infection with arenaviruses in the Americas. Curr. Top. Microbiol. Immunol. 262, 65–74.
Rodrigo, W.W., de la Torre, J.C., Martínez-Sobrido, L., 2011. Use of single-cycle infectious lymphocytic choriomeningitis virus to study hemorrhagic fever arenaviruses. J. Virol. 85, 1684–1695.
Shaltiel, G., Shamir, A., Shapiro, J., Ding, D., Dalton, E., Bialer, M., Harwood, A.J., Belmaker, R.H., Greenberg, M.L., Agam, G., 2004. Valproate decreases inositol biosynthesis. Biol. Psychiatry 56, 868–874.
Snell, N., 1988. Ribavirin therapy for lassa fever. Practitioner 232, 432.
Strecker, T., Eichler, R., Meulen, J., Weissenhorn, W., Dieter Klenk, H., Garten, W., Lenz, O., 2003. Lassa virus Z protein is a matrix protein and sufficient for the release of virus-like particles. J. Virol. 77, 10700–10705 (corrected).

Terbach, N., Williams, R.S., 2009. Structure–function studies for the panacea, valproic acid. Biochem. Soc. Trans. 37, 1126–1132.
Tokuoka, S.M., Saiardi, A., Nurrish, S.J., 2008. The mood stabilizer valproate inhibits both inositol- and diacylglycerol-signaling pathways in *Caenorhabditis elegans*. Mol. Biol. Cell 19, 2241–2250.
Urata, S., Ngo, N., de la Torre, J.C., 2012. The PI3K/Akt pathway contributes to arenavirus budding. J. Virol. 86, 4578–4585.
Urata, S., Noda, T., Kawaoka, Y., Yokosawa, H., Yasuda, J., 2006. Cellular factors required for Lassa virus budding. J. Virol. 80, 4191–4195.
Urata, S., Yasuda, J., de la Torre, J.C., 2009. The z protein of the new world arenavirus tacaribe virus has bona fide budding activity that does not depend on known late domain motifs. J. Virol. 83, 12651–12655.
Vazquez-Calvo, A., Saiz, J.C., Sobrino, F., Martin-Acebes, M.A., 2011. Inhibition of enveloped virus infection of cultured cells by valproic acid. J. Virol. 85, 1267–1274.
Venkataramani, V., Rossner, C., Iffland, L., Schweyer, S., Tamboli, I.Y., Walter, J., Wirths, O., Bayer, T.A., 2010. Histone deacetylase inhibitor valproic acid inhibits cancer cell proliferation via down-regulation of the alzheimer amyloid precursor protein. J. Biol. Chem. 285, 10678–10689.
Weber, E.L., Buchmeier, M.J., 1988. Fine mapping of a peptide sequence containing an antigenic site conserved among arenaviruses. Virology 164, 30–38.
Wittenburg, L.A., Bisson, L., Rose, B.J., Korch, C., Thamm, D.H., 2011. The histone deacetylase inhibitor valproic acid sensitizes human and canine osteosarcoma to doxorubicin. Cancer Chemother Pharmacol 67, 83–92.
Wolf, M.C., Freiberg, A.N., Zhang, T., Akyol-Ataman, Z., Grock, A., Hong, P.W., Li, J., Watson, N.F., Fang, A.Q., Aguilar, H.C., Porotto, M., Honko, A.N., Damoiseaux, R., Miller, J.P., Woodson, S.E., Chantasirivisal, S., Fontanes, V., Negrete, O.A., Krogstad, P., Dasgupta, A., Moscona, A., Hensley, L.E., Whelan, S.P., Faull, K.F., Holbrook, M.R., Jung, M.E., Lee, B., 2010. A broad-spectrum antiviral targeting entry of enveloped viruses. Proc. Natl. Acad. Sci. USA 107, 3157–3162.
Xu, X., Muller-Taubenberger, A., Adley, K.E., Pawolleck, N., Lee, V.W., Wiedemann, C., Sihra, T.S., Maniak, M., Jin, T., Williams, R.S., 2007. Attenuation of phospholipid signaling provides a novel mechanism for the action of valproic acid. Eukaryot. Cell 6, 899–906.